Available online at www.sciencedirect.com
ScienceDirect
Sensors and Actuators B 119 (2006) 632–641
SENSORS AND ACTUATORS B CHEMICAL
www.elsevier.com/locate/snb

Electrochemical, microgravimetric and AFM studies of polythionine films Application as new support for the immobilisation of nucleotides

V. Ferreira, A. Tenreiro, L.M. Abrantes *

CQB, Departamento de Química e Bioquímica, Faculdade de Ciências da Universidade de Lisboa, Campo Grande, 1749-016 Lisboa, Portugal

Received 20 October 2005; accepted 10 January 2006
Available online 21 February 2006

Abstract

The experimental conditions for the thionine potentiodynamic electropolymerisation in acidic media are optimised in order to achieve polythionine (PTN) modified electrodes with high stability and reproducible redox behaviour in acidic and biological compatible media. The data obtained by cyclic voltammetry and electrochemical quartz crystal microbalance (EQCM) show that under the selected conditions, polythionine films growth, presents a non-linear relation between mass and electroactivity which suggests structural changes during electropolymerisation, that are corroborated by atomic force microscopy (AFM). The pH effect in the redox switching of PTN films is studied in solutions with pH from 1.3 to 12 where two processes with different dependence on protons occurs in the interval from 5.5 to 9, indicating a complex behaviour. PTN redox conversion in acidic media is film thickness sensitive and a non-permselective behaviour is found in acidic and neutral media, being the mass change dependent on the electrolyte nature. The presence of free amino functions in the polymer structure enable the nucleotide immobilisation by adsorption and covalent attachment, which was simultaneously monitored by EQCM and open circuit potential. The nucleotidic phosphate groups reactivity is enhanced by adding coupling agents leading to an higher amount of mass immobilisation.

Keywords: Polythionine modified electrodes; Electrochemical quartz crystal microbalance; Atomic force microscopy; Nucleotides immobilisation

1. Introduction

Conducting polymers have been widely studied due to their potential applicability in fields like catalysis, electronic devices and sensor and biosensors design [1]. Their ability to enhance electron transfer along with good sensitivity and versatility has attracted much interest in the use of conducting polymer films, namely polypyrrole, polythiophene and polyaniline, as suitable matrices for biomolecules immobilisation [2,3]. For this purpose, the presence of free functional groups, appropriate for the interaction with biomolecules, provide further advantage.

Functionalised polymer films can be prepared by direct electropolymerisation of functionalised monomers [3,4] or by chemical post-functionalisation of the deposited polymer [5,6]; providing the free functional group is kept after the polymer electrosynthesis, the first route is a promising approach to enable a film formation with specific interaction sites [7–9].

It is known that the use of polymer films able to mediate a catalytic response, is advantageous over the use of mediators in solution. The electropolymerisation of redox mediators has been used to introduce highly efficient redox centers into polymeric system such as polyviologens [10] and phenazine, phenoxazine and phenothiazine derivatives [11–13]. Among the phenothiazine monomers, thionine is a promising material since it contains two amino groups in the α positions and can be electrochemically polymerised by potentiodynamic methods, from acidic [14–19] to neutral [20,21] and slightly alkaline media [12,22,23] and onto different substrates as gold [12,14,15,23,24], platinum [17,18] and carbon [19–21]. Polythionine modified electrodes have been used for the development of catalytic biosensors with enzyme immobilisation by cross-linking [20] or using a Nafion membrane [21]. An electropolymerisation mechanism similar to polyaniline has been proposed in the literature [12,13,22], due to the presence of primary amine electron-donating groups and at least one non-substituted *ortho* or *para* position in the aromatic ring. In this case, it occurs the formation of a stable single charged cation-radical, upon monomer irreversible oxidation at fairly positive potential, just

* Corresponding author. Tel.: +351 21 7500890; fax: +351 21 750 00 88.
E-mail address: luisa.abrantes@fc.ul.pt (L.M. Abrantes).

0925-4005/$ – see front matter © 2006 Elsevier B.V. All rights reserved.
doi:10.1016/j.snb.2006.01.024

before oxygen evolution [12,22]. Although polythionine (PTN) structure is not completely known, spectroscopy studies point to secondary amino bridges between two monomer units and free amino functions in the polymer structure [12,14,22].

PTN characterisation has included electrochemical techniques (cyclic voltammetry and chronoamperometry), electrochemical quartz crystal microbalance (EQCM), ellipsometry, and spectroscopy (UV–vis and infrared), in different aqueous media from acidic to slightly alkaline revealing electroactive and stable responses. The electrochemical behaviour of PTN films is pH dependent [20,21] and the redox switching influenced by the nature and concentration of the electrolyte not verifying the permselective model, as shown by the EQCM studies, reported by Hillman and co-workers [15,16,24,25].

In this work, the results of a detailed investigation on the effect of the electropolymerisation parameters upon the formation of PTN polymer films, electroactive and stable both in acidic and biological media, are analysed aiming to select the optimal conditions for the preparation of a base for biomolecules immobilisation. The morphology and redox behaviour of the so-obtained polythionine modified electrodes, displaying free amino functions, is presented; the films are used as matrix for nucleotide immobilisation achieved by specific interaction or covalent attachment.

2. Experimental

Electrochemical experiments were performed with an IMT Electrochemical Interface and a DEA332 Digital Electrochemical Analyser connected to a computer for data acquisition (VoltaMaster2 software). A three-compartment cell, with a polycrystalline Pt disk working electrode (0.181 cm^2 geometrical area), a Pt foil counter-electrode and a saturated calomel reference electrode (SCE), was used.

The electrochemical quartz crystal microbalance (EQCM) experiments were performed with a frequency analyser (CH Instruments model 420), in a single compartment cell. The working electrode was an 8 MHz AT-cut quartz crystal coated with 1000 Å Pt (0.2 cm^2 geometrical area), a Pt wire as counter electrode and a SCE.

The morphological characterisation of polythionine films (PTN) was performed by atomic force microscopy (AFM) ex situ, *tapping* mode, at an atomic force microscope (Nanoscope IIIa Multimode—Digital Instruments).

PTN were potentiodynamically grown on a Pt working electrode by cycling the potential at a scan rate, $\nu = 20\,mV\,s^{-1}$ between 0 and 1.15 V versus SCE in a 0.05 mol dm^{-3} H_2SO_4 (Fluka, p.a.) solution containing 50 μmol dm^{-3} of thionine acetate (Fluka). Prior to all measurements the solutions were deaerated with N_2 for 15 min.

The polymer layers were washed with monomer free solution, H_2SO_4 0.05 mol dm^{-3} and characterised electrochemically (by cycling the potential at 20 mV s^{-1}) in a wide range of pH values: H_2SO_4 0.05 mol dm^{-3} (pH 1.3), 0.1 mol dm^{-3} sodium phosphate solutions (di-sodium hydrogen phosphate and sodium dihydrogen phosphate, Merck, p.a.) with pH from 5.5 to 12 and 0.05 mol dm^{-3} MES (pH 6.6) (2-morpholinoethanesulfonic acid, Duchefa-Biochemie, >99%). The polythionine films will be referred as PTN *n*/*ν*, where *n* represents the number of potential cycles and *ν* is the sweep rate used in the electropolymerisation.

The immobilisation of biomolecules, deoxyguanosine-triphosphate (dGTP) or 20-mer deosyguanosine oligonucleotide, 5′-phosphate modified (dG20-P) (Invitrogen Technologies), was carried out by adsorption (procedure A) or covalent attachment plus adsorption (procedure B) and followed by the EQCM frequency changes. The PTN films were immersed in a 0.05 mol dm^{-3} MES solution (2 mL) to which the nucleotides were added with a micro-syringe. For the procedure B, a 0.05 mol dm^{-3} MES solution (2 mL) containing 0.010 mol dm^{-3} *N*-hydroxysuccinimide (NHS) (Sigma) and 0.05 mol dm^{-3} *N*-(3-dimethylaminopropyl)-*N*′-ethylcarbodiimide hydrochloride (EDC) (Sigma Ultra) was used. All the solutions were prepared with Milli-Q water.

3. Results and discussion

3.1. Potentiodynamic electropolymerisation of thionine in acidic media

The current–voltage behaviour in the course of potentiodynamic electropolymerisation of polythionine at a platinum electrode (80 cycles, $\nu = 20\,mV\,s^{-1}$) is presented in Fig. 1. In the first potential sweep, with the initial potential at the open circuit potential ($E_{OCP} = 0.5$ V), the irreversible oxidation of thionine on platinum occurs at potentials higher than 1.0 V, with the formation of cations-radical, which probably yields an isomeric dimmer, as reported for amino substituted azines [13]. The oligomers deposition on the electrode surface may occur over a PtO layer [17,18] and no nucleation is observed since thionine adsorbs reversibly on platinum [18]. During the following cycles, a small increase in the oxidation current at 1.150 V is observed; the monotonic increment in the reduction and oxidation peaks current, at approximately 0.185 and 0.220 V, respectively, indicates the growth of electroactive PTN.

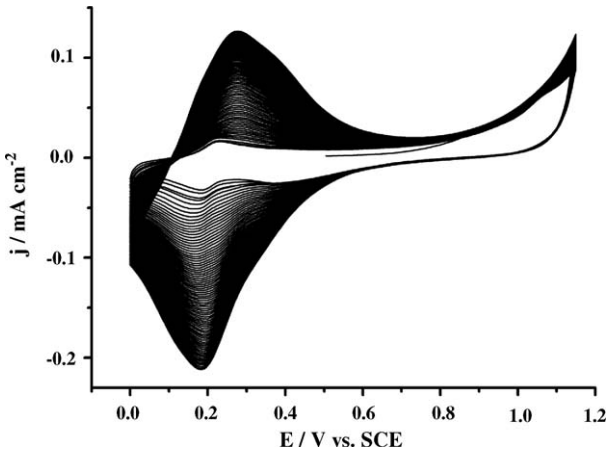

Fig. 1. Cyclic voltammograms (80 cycles) of the electropolymerisation of polythionine in 50 μmol dm^{-3} thionine and 0.05 mol dm^{-3} H_2SO_4 on platinum, $\nu = 20\,mV\,s^{-1}$.

Table 1
Electrochemical data obtained from the voltammograms of the characterisation of PTN films grown under different experimental conditions

E_{al} (V)	ν (mV s^{-1})	n	Q_{ox} (mC cm^{-2})	Q_{red} (mC cm^{-2})	Q_{ox}/Q_{red}	E_p^a(V)	E_p^c(V)	ΔE_p (V)
1.100	20	80	0.315	0.322	0.98	279.2	201.2	78.0
1.150	20	20	0.406	0.306	1.33	276.8	225.8	51.0
		40	0.616	0.466	1.32	271.3	209.7	61.6
		80	0.751	0.803	0.94	262.7	167.2	95.5
	50	80	0.419	0.445	0.94	248.3	153.9	94.4
	100		0.312	0.281	1.11	245.6	167.4	78.2
1.200	20	80	0.427	0.410	1.04	275.1	156.0	119.1
1.230			0.277	0.280	0.99	243.7	163.5	80.2
1.250			0.160	0.202	0.79	258.0	169.5	88.5

E_{al}: anodic limit potential in the electropolymerisation; ν: electropolymerisation sweep rate; n: number of potential cycles; Q: oxidation (ox) and reduction (red) charges obtained from the PTN films characterisation by cyclic voltammetry at a sweep rate of 20 mV s^{-1}; Q_{ox}/Q_{red}: ratio between oxidation and reduction charges; E_p: anodic (a) and cathodic (c) peak potentials; ΔE_p: difference between the anodic and cathodic peak potentials.

It includes the homogeneous redox reaction of the monomer in solution, overlaid with the PTN film redox switching.

Polythionine films formed with different anodic potential limit, sweep rate and number of potential cycles were prepared, rinsed with electrolyte and characterised in monomer free solution, aiming to select the experimental conditions for the potentiodynamic electropolymerisation of thionine in acidic media leading to higher electroactivity of the PTN films. Table 1 presents the obtained electrochemical characterization parameters. The oxidation (Q_{ox}) and reduction (Q_{red}) charges was seen to increase with the anodic limit potential (E_{al}) up to 1.150 V and the number of potential cycles (n) and with the decrease in the sweep rate (ν) between 100 and 20 mV s^{-1}, pointing out the conditions for the formation of the highest amount of electroactive polymer onto the platinum surface, as underlined in the table. It is worthwhile to note that a decrease in electroactivity was observed for PTN produced with more than 80 potential cycles. It can also be seen in Table 1 that to the highest charges involved in the polymer redox conversion corresponds the largest difference of anodic and cathodic peak potentials, ΔE_p, suggesting that structural changes occur in the course of the polymer thickening.

Under the selected experimental conditions, the PTN electrosynthesis has been monitored by EQCM. For the frequency variations treatment, a rigid layer behaviour of the deposited film has been assumed and thus using the Sauerbrey equation [26] a negative frequency shift of 1 kHz equals an electrode-mass increase of 7 μg. From the changes in the resonant frequency of the microbalance during the electropolymerisation cycles, it was possible to observe that the mass increases linearly with the number of cycles, as shown in Fig. 2.

Surface coverage of electroactive sites, Γ, calculated from the film oxidation charge by assuming a two-electron process, is plotted against the deposited PTN mass after 20, 40 and 80 potential cycles, as represented in Fig. 3. In spite of the referred linearity, the electroactivity of PTN films with different thickness does not follow the mass changes, tending to a plateau. This fact can be related to the already mentioned structural changes occurring on the course of the PTN electropolymerisation, which is a possible cause to the lower conductivity of the film [27].

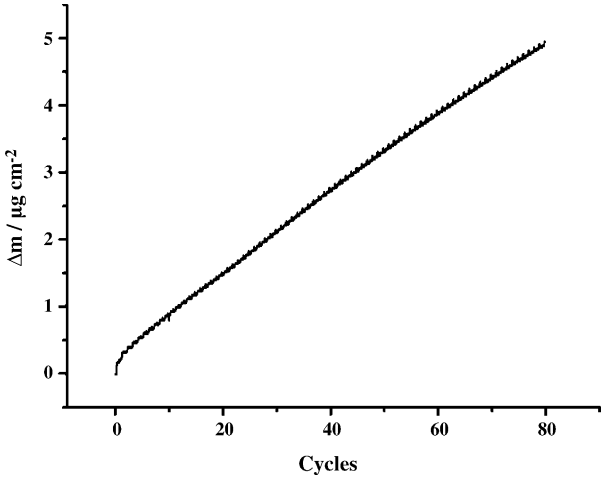

Fig. 2. Δm/cycles potentiodynamic profile registered during the electropolymerisation of PTN film (80 cycles, between 0 and 1.150 V) on Pt electrode from a 50 μmol dm^{-3} thionine in 0.05 mol dm^{-3} H_2SO_4 solution; $\nu = 20$ mV s^{-1}.

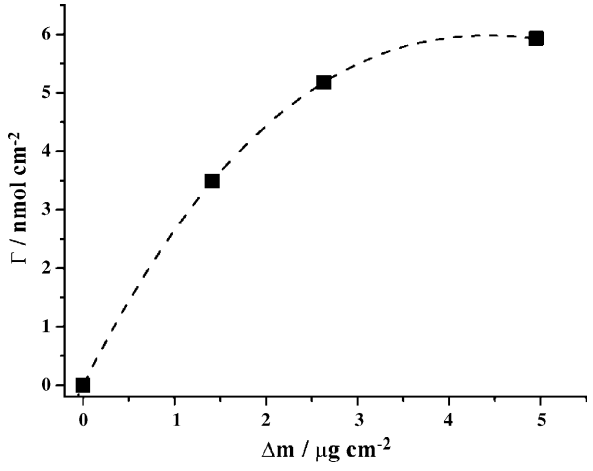

Fig. 3. Surface coverage of electroactive sites and mass deposited on a Pt electrode relation for the potentiodynamic electropolymerisation of PTN films with distinct thickness (20/20, 40/20 and 80/20).

3.2. Electrochemical characterisation of PTN films

As observed for other polymers [11,13], the electrochemical behaviour of PTN films, is pH dependent. It has been reported [20,21] that PTN potentiodynamically grown on screen-printed and glassy carbon electrodes show, in solutions with pH between 6 and 8, a potential decrease of 55 mV/pH, in agreement with the Nernstian value (59 mV) for a two-electron/two-proton process. However, PTN redox switching mechanism it not completely established.

The presence of more than one pair of redox waves in electroactive polymer characterisation has also been detected in other systems such as poly(methylene blue) [13]. The process occurring at more positive potentials was assigned to be due to changes in the aromatic rings which, reducing the donating character of the nitrogen atom, induce the potential shift. The redox pair at more negative potentials was suggested to be due to monomer-type conjugation also present in the polymer [28]. This kind of conjugation, likely arising from the monomer molecules adsorbed on the polymer by S–S bonds, increases the electronic density of the aromatic system and induces the potential shift in the cathodic direction. The formation of benzidine-type bonds by ring-to-ring coupling during the electropolymerisation of azines with primary amino groups as it occurs in polyaniline, has also been reported [22].

The electrochemical characterization of PTN 80/20 in solutions with a wide range of pH values, at pH 1.3 (H_2SO_4) and from 5.5 to 12 (phosphate solutions), Fig. 4, has shown stability and high electroactivity in solutions with pH range from 1.3 to 9. Due to the loss of electroactive sites with increasing pH, in more alkaline media, lower electroactivity was observed which is in agreement with electron transfer between neighbouring redox sites accompanied by proton transfer, i.e., the deprotonation of the polymer reduce the electron transfer rate [27].

Two redox processes can be indentified at pH higher than 5.5 (Fig. 4) which are possibly overlaid in acidic media where only one pair of redox peaks is observed. Among those, the process at more negative potential (I) exhibits pH dependency: the oxidation (I) shifts to less negative potentials with pH decrease by 30 mV/pH between 12 and 7 and 65 mV/pH between 7 and 5.5, which are close to the expected Nernstian values of 29.5 and 59 mV for a one-proton/two-electron and two-electron/two-proton processes, respectively. From pH 5.5 down to 1.3, the oxidation potential shifts by 90 mV/pH, which represents a

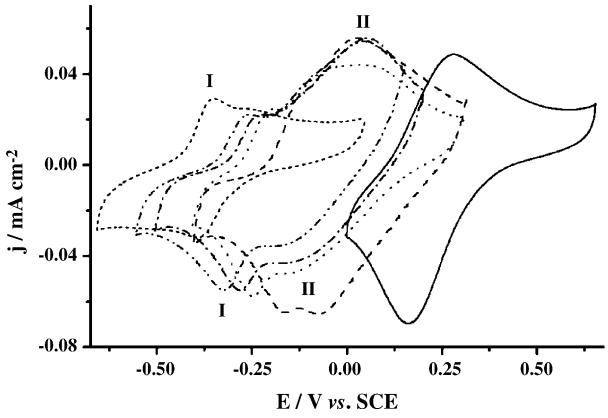

Fig. 4. Cyclic voltammograms of the PTN 80/20 films characterisation in (—) H_2SO_4 0.05 mol dm^{-3} (pH 1.3) and in 0.1 mol dm^{-3} phosphate solutions with different pH values: 5.5 (– – –), 7 (· · ·), 8 (– · – · –), 9 (– · · – · · –) and 12 (- - -); $\nu = 20$ mV s^{-1}.

three-proton/two-electron process. This result differs from the previously proposed in the literature [14] but is in agreement with the reaction scheme represented by Hillman and co-workers [15,17] for the redox switching process occurring in polythionine films at pH less than 5. Moreover, it may mean that both the heterocyclic nitrogen and the nitrogen ring-bridging atoms must be protonated in this media despite of the pK_a of the thionine primary amino groups be less than −1. Azine rings reduction leads to the amino groups protonation in azine containing primary amino which reinforces the three-proton/two-electron mechanism [27]. The second oxidation process (II), at least in the pH interval from 5.5 to 9, appears to be pH independent with no protons taking part on it. On the other hand, the reduction peak (II) seems to have some pH dependency, being shifted to more negative potentials as the pH increases. Table 2 summarizes the potential shift of the anodic and cathodic processes with the increase in solution pH. Besides the protons participation being pH dependent, the oxidation and reduction peaks (I) do not present the same behaviour. For the pH intervals between 1.3 and 5.5, 5.5 and 7 and 7 and 9, a 90 mV/pH (three-proton/two-electron process), 60 mV/pH (two-proton/two-electron process) and 30 mV/pH (one-proton/two-electron process) relations were respectively observed. In the pH range from 9 to 12, while for the oxidation peak (I) a 30 mV/pH (one-proton/two-electron process) dependency was found, for the reduction peak (I) the potential shift was 20 mV/pH (less than one-proton/two-electron

Table 2
Anodic and cathodic peaks potentials of PTN 80/20 films in solutions with different pH

PTN 80/20		E_p^a(V)		E_p^c(V)		ΔE_p (V)	
Solution	pH	(I)	(II)	(I)	(II)	(I)	(II)
H_2SO_4 0.05 M	1.3	0.263		0.167		0.096	
Phosphate solutions 0.1 M	5.5	≈−0.115	0.014	−0.175	−0.058	≈60	72
	7	−0.213	0.005	−0.250	≈−0.143	37	≈148
	8	−0.245	0.059	−0.283	≈−0.158	38	≈217
	9	−0.273	0.038	−0.319	≈−0.185	46	≈223
	12	−0.360	≈−0.272	−0.379	Not observed	19	–

E_p: anodic (a) and cathodic (c) peak potentials; ΔE_p: difference between the anodic and cathodic peak potentials.

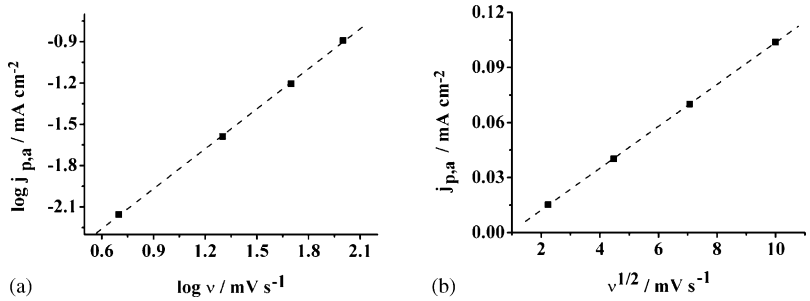

Fig. 5. Plot of the peak current density and sweep rate for polythionine films with different thickness in H_2SO_4 0.05 mol dm^{-3}: (a) PTN 20/20 and (b) PTN 80/20.

process). This may suggest that the cathodic process is complex and takes place in two steps with distinct protons contribution.

Also shown in Table 2, the lower ΔE_p values observed for the redox process (I), support its assignment to protons transfer, which must display faster kinetics than other species, since they may move within the polythionine film via a Grotthus-type process [27] with water molecules and/or amine sites on the polymer, by intermolecular acid/base reactions. This observation is also in agreement with the above mentioned hypothesis of this process being related to monomer-type conjugation present in the polymer [28], since it is pH dependent. On the other hand, oxidation process (II) showed pH independence in the pH range from 5.5 to 9, and much higher ΔE_p. The peaks separation reflect the slower electron transfer, as previously referred, and the stabilisation of the positive charge of the sulfur atom in the phenothiazine ring by the hydroxide anions from the solution [28,29].

In acidic media, the redox switching of PTN films is thickness sensitive, as depicted in Fig. 5. For PTN 20/20 the peak current density presents a linear relationship with the sweep rate but in the case of PTN 80/20 a linear dependence of $\nu^{1/2}$ was found. The data indicates that the charge transport process in the polymer changes from electron transfer to diffusion control with film thickening.

3.3. EQCM polythionine characterisation

Fig. 6 illustrates the simultaneously recorded voltammetry and EQCM data for PTN films with different thickness, PTN 20/20, PTN 40/20 and PTN 80/20, at 20 mV s^{-1} scan rate in H_2SO_4 0.05 mol dm^{-3} and in 0.05 mol dm^{-3} MES solutions. As expected, in both media, the electroactivity (Fig. 6a and b) and the variations in the frequency (Fig. 6a′ and b′) depend on the film thickness.

It was reported by Hillman and co-workers [15,16,24,25] that the permselective model cannot be applied to this type of redox polymers, since the mass changes observed during the redox switching of the films are not in agreement with it and are influenced by the nature and concentration of the electrolyte. Decoupling between charge and mass transfer and the

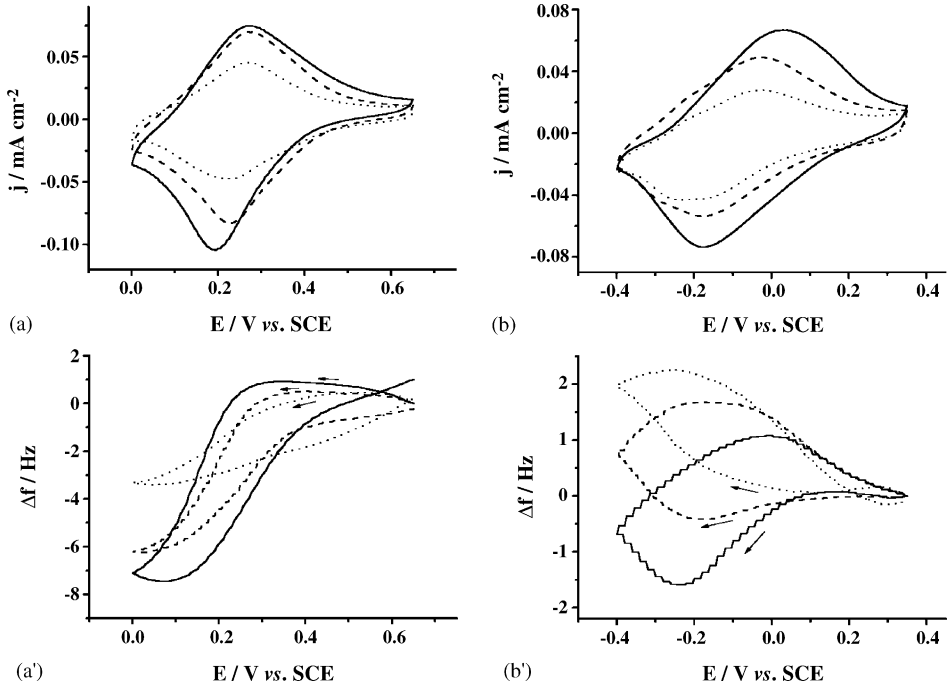

Fig. 6. Cyclic voltammograms and frequency/potential profiles of the (···) PTN 20/20, (– – –) PTN 40/20 and (—) PTN 80/20 characterisation in 0.05 mol dm^{-3} H_2SO_4 (a and a′) and in 0.05 mol dm^{-3} MES solution (pH 6.6) (b and b′); $\nu = 20$ mV s^{-1}.

Table 3
Experimental and calculated mass changes for different thickness PTN films redox switching in acidic media

Film	Δm_{exp} (ng cm^{-2})	Δm_1 (ng cm^{-2})	Δm_2 (ng cm^{-2})
PTN 20/20	23.6	346	7.0
PTN 40/20	46.8	513	10.0
PTN 80/20	55.3	587	11.8

Δm_{exp}: observed mass change during the redox switching of the film; Δm_1: calculated mass change assuming a three-protons/two-electrons process; Δm_2: calculated mass change assuming a two-protons/two-electrons process.

Table 4
Experimental and calculated mass changes for different thickness PTN films redox switching in neutral media

Film	$\Delta m_{exp\,1}$ (ng cm^{-2})	$\Delta m_{exp\,2}$ (ng cm^{-2})	Δm_3 (ng cm^{-2})	Δm_4 (ng cm^{-2})
PTN 20/20	−4.1	−9.6	−527	5.5
PTN 40/20	3.5	−8.4	−967	10.1
PTN 80/20	11.5	−6.3	−1255	13.1

Δm_{exp}: observed mass changes (1 and 2) during the redox switching of the film; Δm_3: calculated mass change assuming an one-proton/two-electron process; Δm_4: calculated mass change assuming a two-proton/two-electron process.

electroneutrality requirements primarily satisfied by protons, in acidic media, due to their easier movement as compared with other ions have also been suggested by the same authors. Indeed, these polymers may contain counter-ion sources, which contributes to differences between experimental and expected mass changes. Moreover, the solvation of charged species and the thermodynamic equilibrium may be only slowly established. However, information about the effect of the solution pH and of PTN films thickness on the mass change during the redox switching is still scarce, and the present study was developed aiming to give some contribution on this issue. The obtained data were compared with the expected values according to the reaction schemes proposed in the literature, in acidic and neutral media.

In acidic media, according to a three-proton/two-electron redox mechanism, suggested by the above discussion on the results of the pH study and reported in the literature [15], upon reduction the PTN film acquire an extra counter-ion for the charge compensation. In this way, a mass increase is expected and was experimentally observed as can be seen in Fig. 6a′. The mass change expected in this media, Δm_1, was calculated from the surface coverage of electroactive sites (Γ), assuming that three protons and an extra counter-ion are involved. As represented in Table 3, the observed, Δm_{exp}, mass increase in the reduction did not come up to the expected value. However, comparing the experimental mass change and the mass expected according with a two-proton/two-electron mechanism, Δm_2, where no protonation of the nitrogen-bridging atom occurs [14] and no counter-ion is required to enter the film, Δm_{exp} and Δm_2 are closer.

In neutral media, 0.05 mol dm^{-3} MES solution, the observed mass change is lower than in acidic media and two domains can be distinguished in Fig. 6b′: during the cathodic scan, up to about −0.2 V, the frequency variation appear to be film thickness sensitive but at more negative potentials a similar slope is obtained for the three films. Although for the reduction of PTN 20/20 it is only detected a mass decrease, different slopes fits the mass change with potential, one from the anodic potential limit (0.35 V) to −0.188 V and another from this to the cathodic potential (−0.4 V), corresponding to a mass decrease of 4.1 and 9.6 ng cm^{-2}, respectively. In the case of thicker films, PTN 40/20 and 80/20, an initial mass increase from the anodic potential limit down to −0.228 and −0.242 V, respectively, followed by a mass decrease are observed. The experimental ($\Delta m_{exp\,1}$ and $\Delta m_{exp\,2}$) and calculated mass changes (Δm_3), are contrasted in Table 4. Δm_3 was obtained by assuming a one-proton/two-electron process, which implies that without any positive charge within the film, the counter-ion present in the oxidised state may egress the film. However, counter-ions may not need to egress out of the film during reduction if they are able to form ion-pairs or if solvated by water molecules ingressing the film, which leads to its mass increase. On the other hand, assuming a two-proton/two-electron mechanism, the experimental and expected mass (Δm_4) changes become closer (Table 4). From the present analysis it is expected that the redox switching of PTN films in neutral media is described by a mixture of both mechanisms and the non-permselective behaviour of polythionine films, in both media, appears to be confirmed.

3.4. Morphological characterisation by AFM

The PTN 20/20, 40/20 and 80/20 modified platinum electrodes were examined in air by *tapping* mode AFM and the obtained 2 μm × 2 μm AFM images and the corresponding profiles are presented in Fig. 7. The topographic images of PTN 20/20 film, presented in Fig. 7a, show the presence of a compact polymeric matrix of small globular features with diameter of ca. 20 nm and nodules spread throughout all surface with typical size ranging from ca. 30 to 70 nm, which may be related to the subsequent formation of a second polythionine layer with distinct structure, as supported from the electrochemical data (Γ versus n) presented in Fig. 3. Increasing the number of the potential cycles in the electropolymerisation, part of the globular features aggregate, as illustrated in Fig. 7b. It is possible to observe the formation of irregular sized and shaped but compact domains with film thickening, which become clearly visible for the film grown with 80 cycles, Fig. 7c. The rms roughness (R_q) average values, 3.3 and 3.8 nm, obtained for 20/20 and 40/20 films, respectively, are similar. However, in spite of the referred compact domains formation, the thicker film present higher R_q value (5.6 nm), which is due to the presence of plateaus, isolated by pronounced cliffs, when compared with the thinner films, as depicted in the profiles.

3.5. Nucleotides immobilisation on PTN films

Biomolecules immobilisation by adsorption onto modified surfaces that contains free functional groups with affinity to these molecules, as DNA, has been reported [30,31]. Unsal et al. [30] studied the DNA immobilisation onto polyethylenimine (PEI) modified poly(*p*-chloromethylstyrene) (PCMS) particles;

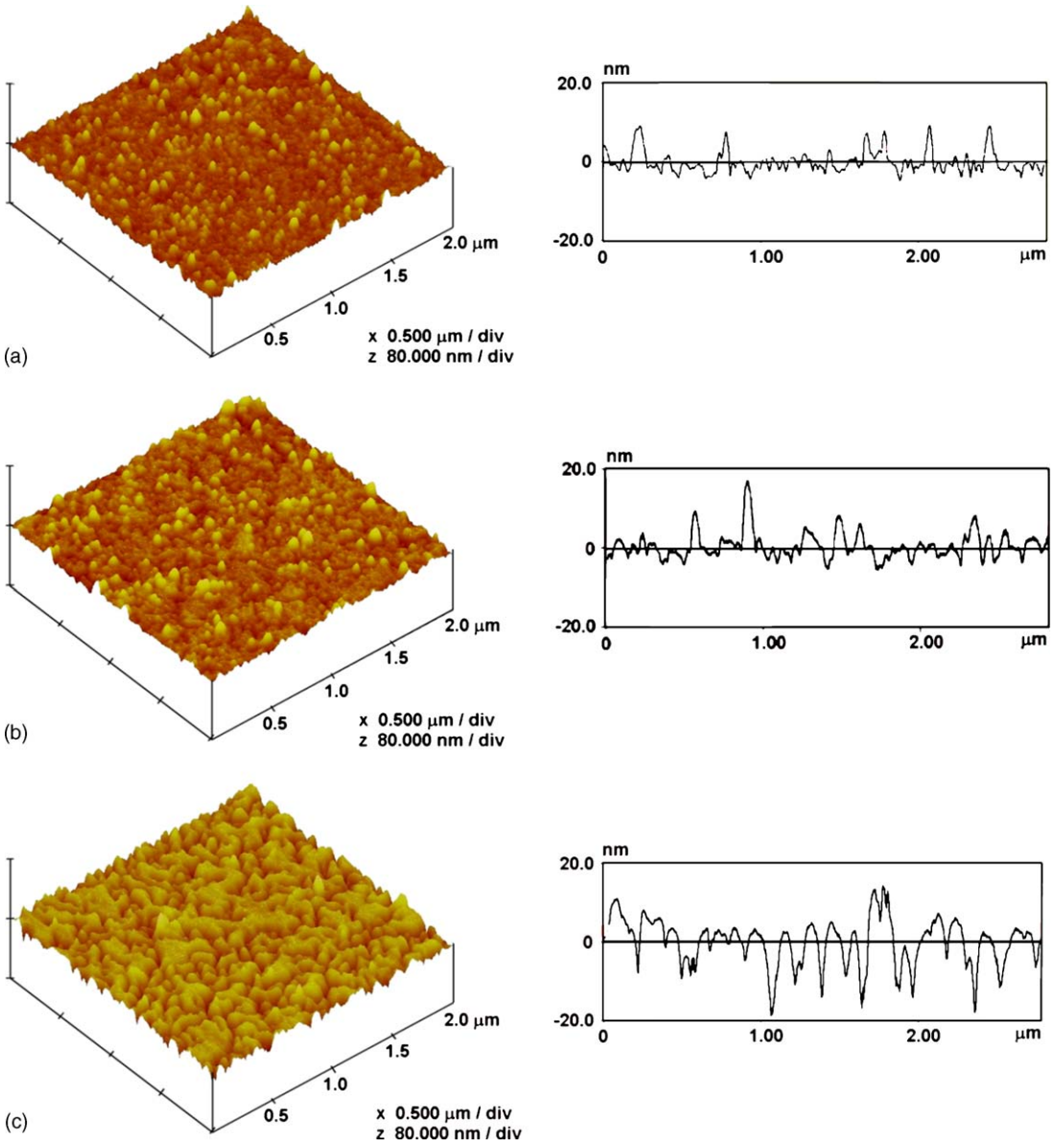

Fig. 7. 3D-processed topographic AFM-tapping mode images and profiles of the polythionine films, PTN 20/20 (a), 40/20 (b) and 80/20 (c).

PEI contains free amino functions, enabling the immobilisation on its surface by interaction with DNA phosphate groups.

Electrostatic interaction between positively charged thionine amine groups and the negative nuclei acids phosphate groups leading to complex formation has also been reported [31]. In this case, the interaction forces are stronger for solutions with low pH; for pH values higher than 2.7, less positive thionine charges result in an weaker interaction. For the nucleotides and DNA sequences immobilization by covalent bonding, the most used coupling agent are NHS and EDC [9,32,33]. The presence of appropriated free functions in the polymer structure enables, through the carbodiimide chemistry, the covalent coupling between the nucleotide phosphate groups, activated by the NHS/EDC agents, and the polythionine amino groups. EDC is a water-soluble carbodiimide derivative which catalyses the formation of the amide bonding between phosphate groups (or carboxylic acids) and amines, by activating the phosphate with an *o*-urea derivative formation. This rapidly reacts with nucleophiles, as amines. NHS is commonly used with EDC for assisting the coupling of the carbodiimide and to lead to a more stable active intermediary. In this case, it is an intermediary ester that reacts with the amino groups leading to a phosphate–amine bond formation.

In the present work, the biomolecule immobilisation onto PTN 80/20 films was performed using two different approaches. In the procedure A, the nucleotide was added to 2 mL of electrolyte solution in the EQCM cell and the interaction is just due to the adsorption of biomolecules on the polymer. For the other approach, procedure B, the biomolecules were added to the MES solution (2 mL) containing the coupling agents (0.01 mol dm^{-3} NHS and 0.05 mol dm^{-3} EDC) and the immobilisation occurs by covalent coupling plus adsorption. The immobilisation was monitored simultaneously by EQCM frequency changes (Δf) and open circuit potential (E_{OCP}) evolution, for 2 h.

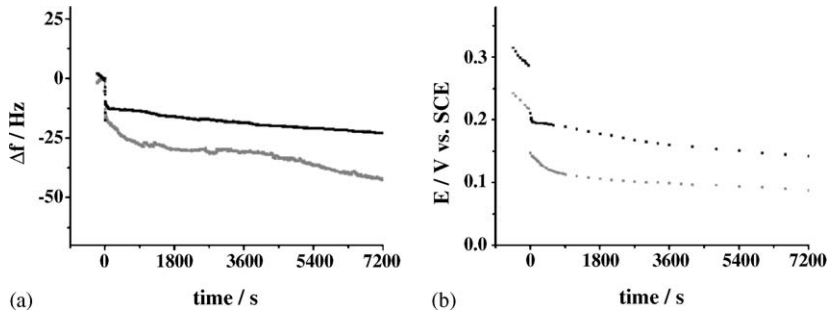

Fig. 8. (a) Frequency and (b) open circuit potential changes during dGTP immobilisation on PTN 80/20 film by (■) adsorption (procedure A) and (■) adsorption plus covalent coupling (procedure B) in 0.05 mol dm^{-3} MES solution.

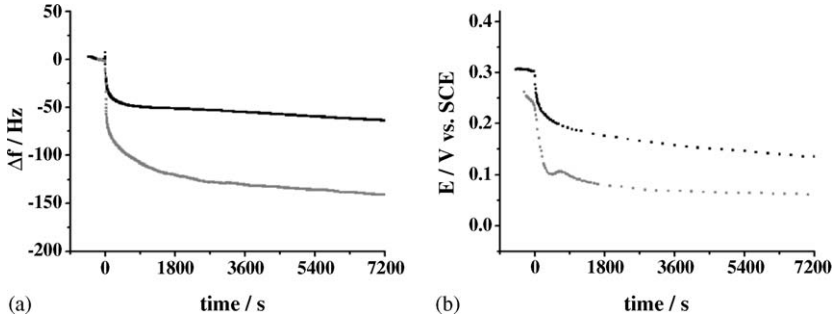

Fig. 9. (a) Frequency and (b) open circuit potential changes during dG20-P immobilisation on PTN 80/20 film by (■) adsorption (procedure A) and (■) adsorption plus covalent coupling (procedure B) in 0.05 mol dm^{-3} MES solution.

The data collected for dGTP and dG20-P immobilisation, in polythionine films by both procedures A and B is presented in Figs. 8 and 9. Sauerbrey equation [26] was used to calculate from the experimental Δf values, the mass deposited, on the modified electrode, Δm presented in Table 5. As expected, the amount of dGTP immobilised by covalent coupling plus adsorption (0.297 μg cm^{-2}) was seen to be twice the observed for simple adsorption (0.158 μg cm^{-2}). A similar relation has been found for the case of dG20-P immobilisation, with a mass increase of 0.442 and 0.978 μg cm^{-2} for adsorption and covalent coupling plus adsorption, respectively.

The calculated mass changes allowed to estimate the surface coverage by biomolecules, Γ, considering the geometrical area (0.2 cm^2) and using the molecular masses of 573.1 g mol^{-1} for dGTP and 6941.0 g mol^{-1} for dG20-P. The theoretical surface coverage for a dGTP monolayer ($\Gamma_{\text{theoretical}} = 0.276$ nmol cm^{-2}) was calculated by assuming the most packed orientation, with the area per molecule equal to 60.1 Å^2.

Table 5
Experimental and calculated data from the dGTP and dG20-P immobilisation by adsorption and covalent coupling plus adsorption

Biomolecules	dGTP		dG20-P	
	A[a]	B[a]	A[a]	B[a]
Δf (Hz)	−22.81	−42.45	−63.60	−140.77
Δm (μg cm^{-2})	0.158	0.297	0.442	0.978
Γ (nmol cm^{-2})	0.276	0.518	0.064	0.141
ΔE_{OCP} (V)	0.145	0.130	0.168	0.173

Δf: experimental immobilisation frequency shift; Δm: mass change; Γ: surface coverage of biomolecules; ΔE_{OCP}: open circuit potential change after biomolecules addition.
[a] Immobilisation procedure.

Comparing the amount of dGTP and dG20-P immobilised by using the same experimental procedure, it was found that the surface coverage of dGTP, was approximately four times larger than the obtained for dG20-P, as shown in Table 5. In this case, the size, orientation on the polymer surface and repulsions between immobilised oligonucleotides may be responsible for the lower surface coverage observed. The theoretical surface coverage for a dGTP monolayer was found to be equal ($\Gamma_{\text{dGTP,A}} = 0.276$ nmol cm^{-2}) or lower ($\Gamma_{\text{dGTP,B}} = 0.518$ nmol cm^{-2}) than the values obtained throughout procedures A and B, respectively. It must be pointed out that the estimation does not take into account the modified electrode surface roughness. In fact, the electrode real area is known to be higher than the geometrical one, but different orientations and the occurrence of repulsions between the biomolecules may also contribute for the mentioned difference. Moreover, the shift of the open circuit potentials, observed in Figs. 8 and 9b, are in agreement with the EQCM results, suggesting an alteration in the interface, very likely due to those interactions.

4. Conclusions

The electroactivity of PTN films strongly depends on the experimental polymerisation conditions, namely the anodic limit potential, sweep rate and number of potential cycles. The possibility to monitor in situ both electropolymerisation and the

biomolecules immobilisation process by EQCM proved to be a suitable method to characterise these systems.

A linear mass increase with number of potential cycles used for the electropolymerisation is observed but the polymer electroactivity tends to a plateau suggesting structural changes during film thickening which are corroborated by the distinct morphological features observed in AFM images. The redox switching of PTN is film thickness dependent, changing from electronic transfer in thin films to diffusion controlled processes in thick films.

The redox switching of PTN 80/20 films in media of different pH appear to be complex, involving two processes in solutions with pH between 5.5 and 9, with distinct dependence on protons. Accordingly, the mass changes observed during the redox switching of PTN films in acidic and neutral media cannot be described by a permselective model and depends on the electrolyte nature, namely the solution pH.

Polythionine films showed a reversible and stable behaviour in acidic and biological compatible media giving the possibility to be employed as supports for the biomolecules immobilisation. The presence of the free amino functions in the polymer structure enabled the covalent attachment of dGTP (0.297 $\mu g\,cm^{-2}$) and dG20-P (0.978 $\mu g\,cm^{-2}$) being the immobilisation enhanced by the presence of the coupling agents.

Acknowledgements

The authors wish to acknowledge Fundação para a Ciência e a Tecnologia, for financial support, project POCTI/ESP/39233/2001 and to Dr. Ana S. Viana – SPM Laboratory (FCUL) – for the AFM images.

References

[1] G. Inzelt, M. Pineri, J.W. Schultze, M.A. Vorotyntsev, Electron and proton conducting polymers: recent developments and prospects, Electrochim. Acta 45 (2000) 2403–2421.
[2] M. Gerard, A. Chaubey, B.D. Malhotra, Application of conducting polymers to biosensors, Biosens. Bioelectron. 17 (2002) 345–359.
[3] S. Cosnier, Biomolecule immobilization on electrode surfaces by entrapment or attachment to electrochemically polymerized films. A review, Biosens. Bioelectron. 14 (1999) 443–456.
[4] N. Lassale, P. Mailley, E. Vieil, T. Livache, A. Roget, J.P. Correia, L.M. Abrantes, Electronically conductive polymer grafted with oligonucleotides as electrosensors of DNA. Preliminary study of real time monitoring by in situ techniques, J. Electroanal. Chem. 509 (2001) 48–57.
[5] R. Korri-Youssoufi, F. Garnier, P. Srivastava, P. Godillot, A. Yassar, Towards bioelectronics: specific DNA recognition based on an oligonucleotide-functionalized polypyrrole, J. Am. Chem. Soc. 119 (1997) 7388–7389.
[6] S. Cosnier, D. Fologea, S. Szunerits, R.S. Marks, Poly(dicarbazole-*N*-hydroxysuccinimide) film: a new polymer for the reagentless grafting of enzymes and redox mediators, Electrochem. Commun. 2 (2000) 827–831.
[7] H. Gu, X. Su, K.P. Loh, Conductive polymer-modified boron-doped diamond for DNA hybridization analysis, Chem. Phys. Lett. 388 (2004) 483–487.
[8] L.D. Tran, B. Piro, M.C. Pham, T. Ledoan, C. Angiari, L.H. Dao, F. Teston, A polytyramine film for covalent immobilization of oligonucleotides and hybridization, Synth. Met. 139 (2003) 251–262.
[9] A. Tenreiro, C.M. Cordas, L.M. Abrantes, Oligonucleotide immobilisation on polytyramine-modified electrodes suitable for electrochemical DNA biosensors, Portug. Electrochim. Acta 21 (2003) 361–370.
[10] K. Kamata, T. Suzuki, T. Kawai, T. Iyoda, Voltammetric anion recognition by a highly cross-linked polyviologen film, J. Electroanal. Chem. 473 (1999) 145–155.
[11] Z. Puskás, G. Inzelt, Formation and redox transformations of polyphenazine, Electrochim. Acta 50 (2005) 1481–1490.
[12] D.D. Schlereth, A.A. Karyakin, Electropolymerization of phenothiazine, phenoxazine and phenazine derivatives: characterization of the polymers by UV–visible difference spectroelectrochemistry and Fourier transform IR spectroscopy, J. Electroanal. Chem. 395 (1995) 221–232.
[13] D.D. Schlereth, W. Schuhmann, H.-L. Schmidt, Spectroelectrochemical characterization of ultra-thin films formed by electropolymerization of phenothiazine derivatives on transparent gold electrodes, J. Electroanal. Chem. 381 (1995) 63–70.
[14] E.I. Sáez, R.M. Corn, In situ polarization modulation-Fourier transform infrared spectroelectrochemistry of phenazine and phenothiazine dye films at polycrystalline gold electrodes, Electrochim. Acta 38 (12) (1993) 1619–1625.
[15] S. Bruckenstein, C.P. Wilde, A.R. Hillman, Transport phenomena accompanying redox switching in polythionine films immersed in aqueous acetic acid solutions, J. Phys. Chem. 94 (1990) 6458–6464.
[16] A.R. Hillman, D.C. Loveday, M.J. Swann, R.M. Eales, A. Hamnett, S.J. Higgins, S. Bruckenstein, C.P. Wilde, Charge transport in electroactive polymer films, Faraday Discuss., Chem. Soc. 88 (1989) 151–163.
[17] A. Hamnett, A.R. Hillman, An ellipsometric study of polymeric thionine films on platinum, J. Electroanal. Chem. 195 (1985) 189–196.
[18] A. Hamnett, A.R. Hillman, A study of the electrochemical growth and optical properties of polymeric thionine films on platinum using ellipsometry, J. Electroanal. Chem. 233 (1987) 125–146.
[19] C. Lee, J. Kwak, L.J. Kepley, A.J. Bard, Polymer films on electrodes. Part 23. Ellipsometric study of the electrochemical redox processes of a thionine film on a glassy carbon electrode, J. Electroanal. Chem. 282 (1990) 239–252.
[20] Q. Gao, X. Cui, F. Yang, Y. Ma, X. Yang, Preparation of poly(thionine) modified screen-printed carbon electrode and its application to determine NADH in flow injection analysis system, Biosens. Bioelectron. 19 (3) (2003) 277–282.
[21] R. Yang, C. Ruan, W. Dai, J. Deng, J. Kong, Electropolymerization of thionine in neutral aqueous media and H_2O_2 biosensor based on poly(thionine), Electrochim. Acta 44 (1999) 1585–1596.
[22] A.A. Karyakin, E.E. Karyakina, H.-L. Schmidt, Electropolymerized azines: a new group of electroactive polymers, Electroanalysis 11 (3) (1999) 149–155.
[23] Y. Xiao, H.-X. Ju, H.-Y. Chen, A reagentless hydrogen peroxide sensor based on incorporation of horseradish peroxidase in poly(thionine) film on a monolayer modified electrode, Anal. Chim. Acta 391 (1999) 299–306.
[24] S. Bruckenstein, C.P. Wilde, M. Shay, A.R. Hillman, D.C. Loveday, Observation of kinetic effects during interfacial transfer at redox polymer films using the quartz crystal microbalance, J. Electroanal. Chem. 258 (1989) 457–462.
[25] S. Bruckenstein, C.P. Wilde, M. Shay, A.R. Hillman, Experimental observations on transport phenomena accompanying redox switching in polythionine films immersed in strong acid solutions, J. Phys. Chem. 94 (1990) 787–793.
[26] S. Bruckenstein, M. Shay, Experimental aspects of use of the quartz crystal microbalance in solution, Electrochim. Acta 30 (10) (1985) 1295–1300.
[27] T. Komura, M. Ishihara, T. Yamaguchi, K. Takahashi, Charge-transporting properties of electropolymerized phenosafranin in aqueous media, J. Electroanal. Chem. 493 (2000) 84–92.
[28] A.A. Karyakin, A.K. Strakhova, E.E. Karyakina, S.D. Varfolomeyev, A.K. Yatsimirsky, The electrochemical polymerisation of methylene blue and bioelectrochemical activity of the resulting film, Bioelectrochem. Bioenerg. 32 (1) (1993) 35–43.
[29] J.Y. Ding, P.Y. Shih, C.K. Yin, Photochemically stable fluorescence from hybrid of thionine/silica matrix, Mater. Chem. Phys. 84 (2004) 263–272.
[30] E. Unsal, T. Bahar, M. Tuncel, A. Tuncel, DNA adsorption onto polyethylenimine-attached poly(*p*-chloromethylstyrene) beads, J. Chromatogr. A 898 (2000) 167–177.

[31] X. Long, S. Bi, X. Tao, Y. Wang, H. Zhao, Resonance Rayleigh scattering study of the reaction of nucleic acids with thionine and its analytical application, Spectrochim. Acta Part A 60 (2004) 455–462.
[32] K.M. Millan, S.R. Mikkelsen, Sequence-selective biosensor for DNA based on electroactive hybridization indicators, Anal. Chem. 65 (1993) 2317–2323.
[33] Y.-D. Zhao, D.-W. Pang, S. Hu, Z.-L. Wang, J.-K. Cheng, H.-P. Dai, DNA-modified electrodes. Part 4. Optimization of covalent immobilization of DNA on self-assembled monolayers, Talanta 49 (1999) 751–756.

Biographies

Virgínia Ferreira is a postgraduate research student working towards a MSc degree in applied electrochemistry at the Faculdade de Ciências of Universidade de Lisboa (Portugal), under the supervision of Professor Luisa Maria Abrantes and Dr. Ana M. Tenreiro. She received her graduation in chemistry in 2002 at the Faculdade de Ciências of Universidade do Porto (Portugal). The main focus of her current research is on the development of electrochemical DNA biosensors based on functionalised conducting polymer modified electrodes as support for nucleotides immobilisation.

A.M. Tenreiro is an assistant professor of biology at the Faculdade de Ciências of Universidade de Lisboa. At present she is a researcher at the Interfacial Electrochemistry Group. She has been engaged in the research fields of biosensor and biological electrochemistry, and has recently main research interests in the development of DNA and enzymes biosensors.

L.M. Abrantes is a professor of electrochemistry and the leader of the Interfacial Electrochemistry Group at the CQB, FCUL. Her research is focused on the characterization of the interfacial processes involved in the preparation of modified electrodes, namely the formation and growth of electronically conducting polymers (ECP), self-assembled monolayers (SAMs), electroless metal deposition (EMD), and in the performance of those materials in electrocatalysis and as electrochemical biosensors.